Modeling flow and transport in highly heterogeneous three-dimensional aquifers: Ergodicity, Gaussianity, and anomalous behavior— 1. Conceptual issues and numerical simulations

I. Janković,[1] A. Fiori,[2] and G. Dagan[3]

Received 17 November 2005; revised 3 March 2006; accepted 23 March 2006; published 24 May 2006.

[1] Uniform flow of mean velocity U takes place in a highly heterogeneous, isotropic, aquifer of lognormal conductivity distribution (variance σ_Y^2, integral scale I). A conservative solute is injected instantaneously over an area A_0 at $x = 0$, normal to the mean flow, in a flux-proportional mode. Longitudinal spreading is caused by advection by the fluid velocity and is quantified with the aid of the mass flux $\mu(t, x)$ through fixed control planes at x. An equivalent macrodispersivity is defined in terms of the traveltime variance. The flow and transport are solved numerically in three realizations of the conductivity field with $\sigma_Y^2 = 2, 4, 8$, respectively. The medium is modeled by a collection of a large number $N = 100{,}000$ of spherical inclusions whose conductivities are drawn at random. Transport is simulated by tracking 40,000 particles originating at a large injection area ($A_0 \simeq 2000\ I^2$) and for travel distance $x \leq 121\ I$. It is found that the mass flux has a highly skewed time distribution because of the late arrival of solute particles that are moving through low-conductivity blocks. The tail leads to large values of the equivalent macrodispersivity, which is highly dependent on cutoffs corresponding to the arrival of even 0.999 or 0.995 of the total mass. Furthermore, the tail is nonergodic, as it depends on the plume size. Transport appears to be anomalous in the considered interval, although by the central limit theorem it has to tend asymptotically to Fickianity and Gaussianity.

Citation: Janković, I., A. Fiori, and G. Dagan (2006), Modeling flow and transport in highly heterogeneous three-dimensional aquifers: Ergodicity, Gaussianity, and anomalous behavior—1. Conceptual issues and numerical simulations, *Water Resour. Res.*, *42*, W06D12, doi:10.1029/2005WR004734.

1. Introduction

[2] The mechanism of spreading of solutes (macrodispersion) in transport through porous formations of spatially variable hydraulic conductivity K is dominated by the advective effect related to velocity variations. Considerable research has been carried out in the last two decades in order to investigate the relationship between heterogeneity and transport. In applications, the interest in the problem stems from its relevance to contaminant transport in aquifers. From a theoretical standpoint the topic is at the cross road between two central fields of engineering and physics: the solution of the flow problem has common ground with continuum theories of heterogeneous media while that of transport is intimately related to turbulent diffusion. It is therefore quite appropriate to include this topic in the present special issue.

[3] Because of the seemingly erratic spatial variation of K and scarcity of field data, it is customary to model it as a space random function and similarly for flow and transport variables. It is important to emphasize that in hydrological applications (unlike controlled laboratory experiments), there is large uncertainty in characterizing even the statistical structure of K. Thus understanding of the main mechanisms and development of simple, though approximate, models is highly desirable. Sophisticated and complex models, though of theoretical interest, may be of little use in practice in absence of supporting data.

[4] With these goals in mind, we consider here the simplest configuration: K is a three-dimensional isotropic stationary space random function, with $Y = \ln K$ of univariate normal distribution ($\langle Y \rangle = \ln K_G$, $var(Y) = \sigma_Y^2$, K_G geometric mean) while I stands for the finite integral scale of Y; the flow is steady and uniform in the mean (pertinent to natural gradient flow); the plume of the conservative solute is of large transversal dimension as compared to I, to make statistical properties of transport weakly dependent on the particular realization.

[5] In the past numerical and analytical solutions were achieved primarily for weak heterogeneity ($\sigma_Y^2 < 1$); the large body of literature is reviewed in a few books [e.g., *Dagan*, 1989; *Gelhar*, 1994; *Rubin*, 2003]. Numerical solutions for moderate to highly heterogeneous formations were achieved

[1]Department of Civil, Structural and Environmental Engineering, State University of New York at Buffalo, Buffalo, New York, USA.
[2]Dipartimento di Scienza dell'Ingegneria Civile, Universita' di Roma Tre, Rome, Italy.
[3]Department of Fluid Mechanics and Heat Transfer, Tel Aviv University, Tel Aviv, Israel.

0043-1397/06/2005WR004734$09.00

mainly for two-dimensional structures [*Bellin et al.*, 1992; *Salandin and Fiorotto*, 1998; *Wen and Gomez-Hernandez*, 1998; *Zinn and Harvey*, 2003; *Trefry et al.*, 2003].

[6] In the present study we investigate the effect of 3-D heterogeneity, as encountered in aquifer applications. Although useful information may be derived from 2-D solutions, the conclusions may not apply to actual formations [see *Janković et al.*, 2003b]. Besides, we consider high degree of heterogeneity ($\sigma_Y^2 \leq 8$), as found in some aquifers. Beyond such applications, understanding the effect of large σ_Y^2 casts light on the applicability of common approaches, that were developed for weak heterogeneity. Few simulations of three-dimensional flows were carried out in the past [*Tompson and Gelhar*, 1990; *Chin*, 1997] under limiting conditions: relatively small dimension of the solute plume, effect of domain boundaries and limited accuracy of the numerical codes.

[7] Our interest resides in solving flow and transport for a given Y field (in a statistical sense) and we do not refer here to approaches in which transport is not directly related to the underlying permeability field.

[8] The highly accurate numerical solution is derived for a solute plume of large extent (transverse area of $2000I^2$) and for a relatively large travel distance from the source ($121I$). This is achieved by using the structure model we coined as "multi-indicator" in the past: the medium is made up from a large number $N = 10^5$ of blocks of constant K_j ($j = 1, \ldots, N$) that are drawn independently from a lognormal distribution. For simplicity, they are spheres that are submerged in a homogenous matrix of conductivity equal to the effective one. While highly idealized, such a structure may represent, by selecting the radii R, the volume density n and the variance σ_Y^2, any isotropic aquifer of given σ_Y^2 and I. Although multi-indicator model is capable of reproducing any actual covariance structure by adopting specific distributions of conductivities and radii, the present study focuses on constant R. The impacts of the variable radii on flow and transport results are expected to increase as heterogeneity levels are increased. This topic, including the inability of second-order properties of Y ($\langle Y \rangle$, σ_Y^2 and I) to fully capture transport, is deferred to future studies.

[9] There are alternative spatial distributions that satisfy the same constraints (e.g., the multi-Gaussian one; see discussion by *Dagan et al.* [2003]). The great advantage of the adopted structural model is that it permits one to solve flow in large domains and with high accuracy, by the use of the analytic element method [*Strack*, 1989]. We doubt this is feasible at present with the more conventional numerical methods (finite differences, finite elements).

[10] We have solved the same problem previously [*Janković et al.*, 2003a, 2003b]. The main additional features of the present study are rather than concentrating on the second spatial moment and the related macrodispersion, we analyze here the entire longitudinal mass distribution of the plume, with emphasis on its skewness; the domain and plume sizes and the travel distance are larger, permitting us to investigate ergodicity issues and anomalous behavior; the solute injection mode is different (flux proportional rather than uniform); transport is analyzed in terms of BTC (breakthrough curve) at fixed control planes rather than spatial moments. Besides, the approximate semianalytical model is extended in part 2 of the study [*Fiori et al.*, 2006] to describe the complete BTC and the tailing effect.

[11] Our main aim is to achieve a better understanding of the mechanisms affecting transport at high σ_Y^2 and to capture them by simple models. Extension to anisotropic media and to more complex geometries, that resemble actual aquifers, is deferred for future studies.

[12] The plan of the paper is as follows: in section 2 we describe the modeling of the solute plume, and we summarize the definitions of ergodicity, Gaussianity, Fickianity, and anomalous behavior. Section 3 is devoted to the description of the numerical simulations; numerical results are presented in Section 4, and Section 5 concludes the paper. Part 2 of the study [*Fiori et al.*, 2006, hereinafter referred to as P2] presents an approximate semianalytical model and the summarizing discussion of the two parts.

2. Modeling of Plume Mass Arrival and Related Moments and Definition of Ergodicity, Gaussianity, and Anomalous Behavior

[13] The steady flow velocity $\mathbf{V}(\mathbf{x})$ obeys Darcy's law $\mathbf{V} = -(K/\theta)\nabla H$, where $\mathbf{x}(x, y, z)$ is a coordinate vector and H is the pressure head. The effective porosity θ is assumed to be constant and $\mathbf{V}$ satisfies therefore the continuity equation $\nabla.\mathbf{V} = 0$. Boundary conditions are such that the mean velocity $\mathbf{U}(U, 0, 0)$ is constant. The velocity is a stationary random space function that depends in a complex manner on $K(\mathbf{x})$ and on $\mathbf{U}$. A detailed analysis of the Eulerian and Lagrangian velocity fields was presented by *Fiori et al.* [2003], while the present study is focused on transport.

[14] A conservative solute is injected instantaneously on an area A_0, in the plane $x = 0$, normal to the mean flow direction. The distribution of the initial plume mass is described by the relative areal mass function $m_0(\mathbf{a}) = (1/M_0)dM_0/dA_0$, where $\mathbf{a}(a_y, a_z)$ is a coordinate vector in A_0, M_0 is the total mass and $\int_{A_0} m_0(\mathbf{a})d\mathbf{a} = 1$. Two common injection modes are of uniform distribution $m_0 = 1/A_0 = const$ and of flux proportional with $m_0 = [V_x(\mathbf{a})/\overline{V_x}](1/A_0)]$, where $\overline{V_x} = (1/A_0)\int_{A_0} V_x(\mathbf{a})d\mathbf{a}$. While the injection mode affects the plume in the neighborhood of the source for weak heterogeneity [*Demmy et al.*, 1999], it may affect it for a considerable distance for large σ_Y^2. As we shall show in the following, the reason is the large residence time of the solute in zones of low K within A_0. We adopt here the flux-proportional injection mode, which is appropriate to plumes originating from wells that operate at uniform head. The impact of uniform injection for highly heterogeneous formations will be discussed separately in a future publication.

[15] In this article longitudinal transport is investigated with the aid of the mass arrival function $M(t, x)$ at an arbitrary control plane at x, defined as the relative mass of solute that has moved beyond x at time t [e.g., *Rinaldo et al.*, 1989; *Cvetkovic and Shapiro*, 1990; *Cvetkovic and Dagan*, 1994, 1996]. The mass can be related to solute particles trajectories by the simple relationships [*Cvetkovic and Dagan*, 1994]

$$M(t,x) = \int_{A_0} m_0(\mathbf{a})\, H[X(t,\mathbf{a}) - x]\, d\mathbf{a} = \int_{A_0} m_0(\mathbf{a})\, H[t - \tau(x,\mathbf{a})]\, d\mathbf{a} \quad (1)$$

[16] Here $H(x)$ stands for Heaviside unit function ($H(x) = 1$ for $x > 0$, $H(x) = 0$ for $x < 0$) while $\mathbf{x}(x, y, z) = \mathbf{X}(t, \mathbf{a})$ denotes the trajectory of a particle that originates at $\mathbf{x} = \mathbf{a}$ at $t = 0$. We neglect pore-scale dispersion and molecular diffusion so that $d\mathbf{X}/dt = \mathbf{V}(\mathbf{X})$ describes fluid particles trajectories. In turn, $\tau(x, \mathbf{a})$ is the traveltime from the injection plane to the CP (control plane) of a particle originating at $\mathbf{a}$. It can be defined similarly with the aid of the velocity field or by the implicit equation $x - X(\tau, \mathbf{a}) = 0$. In simple words (1) states that the mass arrived at the CP is made up from those particles that have crossed the CP at time t. It is seen that the limiting values are $M(0, x) = 0$ and $M(\infty, x) = 1$. The graph of M as function of t for a fixed x is also known as the BTC (breakthrough curve).

[17] The relative mass flux through the CP [*Cvetkovic and Shapiro*, 1990] is given by differentiation of (1) as follows

$$\mu(t,x) = \frac{\partial M}{\partial t} = \int_{A_0} m_0(\mathbf{a})\, \delta[t - \tau(x,\mathbf{a})]\, d\mathbf{a} \tag{2}$$

where δ is the Dirac function. In the present study we shall characterize longitudinal transport with the aid of μ and its moments

$$\mu_p(x) = \int_0^\infty t^p \mu(t,x)\, dt = \int_{A_0} m_0(\mathbf{a})\, \tau^p(x,\mathbf{a})\, d\mathbf{a} \tag{3}$$

Thus $\mu_0 = 1$ whereas the central temporal moments are defined for $p > 0$ by

$$\begin{aligned} T(x) &= \mu_1 = \int_0^\infty t\mu(t,x)\, dt = \int_{A_0} m_0(\mathbf{a})\, \tau(x,\mathbf{a})\, d\mathbf{a}\ ; \\ \sigma_t^2(x) &= \int_0^\infty (t-T)^2 \mu(t,x)\, dt = \mu_2 - \mu_1^2 \\ S_t(x) &= \frac{1}{\sigma_t^3} \int_0^\infty (t-T)^3 \mu(t,x)\, dt = \frac{\mu_3 + 2\mu_1^3 - 3\mu_1\mu_2}{\left(\mu_2 - \mu_1^2\right)^{3/2}} \end{aligned} \tag{4}$$

[18] These definitions are used in the analysis of numerical simulations results (see section 3).

[19] In a similar manner we can depict the longitudinal spatial spread by the relative mass per unit length

$$m(t,x) = -\frac{\partial M}{\partial x} = \int_{A_0} m_0(\mathbf{a})\, \delta[x - X(t,\mathbf{a})]\, d\mathbf{a} \tag{5}$$

and by the associated spatial moments [see, e.g., *Dagan*, 1989]. The resident concentration $C(\mathbf{x}, t)$ is related to m by $m = (\theta/M_0)\int\int C(x, y, z, t)\, dy\, dz$.

2.1. Ergodic Behavior

[20] While the rigorous definition of ergodicity is mathematically intricate, the one adopted here, of interest in hydrological applications, is as follows: if the one realization spatial sampling of a structural, flow or transport attribute is close to the ensemble distribution and the difference can be reduced by increasing the sampling volume, the process is coined as ergodic.

[21] Ergodicity can be assessed empirically by carrying out Monte Carlo simulations and finding out if the variance of the attribute tends to zero with increasing averaging volume. While repeated numerical simulations are feasible for 2-D or weak heterogeneity, this is prohibitive for 3-D flows and large σ_Y^2. An alternative approximate approach, that is more relevant to hydrological applications, is to model one realization over a large domain and to check whether the attribute mean is affected by a reduction of the averaging volume. This is the approach adopted in the present study.

[22] We have checked for instance that the pdf of the log conductivity Y is approximated very accurately by the histogram of Y_j ($j = 1, \ldots, N$) of the $N = 10^5$ spherical blocks making up the medium. Similarly we found out that the theoretical two-point autocorrelation $\rho_Y(\mathbf{r}) = \langle Y'(\mathbf{x})\mathbf{Y}'(\mathbf{x} + \mathbf{r})\rangle/\sigma_Y^2$, where $Y' = Y - \langle Y\rangle$, is close to the one obtained by spatial averaging (section 3).

[23] In a similar manner we have checked that the space averaged velocity V_x over the entire domain is close to the ensemble mean U and the difference was less than 3% for $\sigma_Y^2 \leq 8$. We therefore regard the numerical simulation for the given realization of the medium, of flow and of the plume as basic configurations to assess ergodic behavior of different transport attributes. It is emphasized that the size of the initial plume here is much larger than in previous investigations [*Tompson and Gelhar*, 1990; *Chin*, 1997], and this is one of the redeeming features of the present study.

[24] As mentioned above, longitudinal transport is investigated here with the aid of the mass flux $\mu(t, x)$ (2) or the BTC $M(t, x)$ (1). Ergodic behavior of this attribute implies that

$$\mu(t,x) \simeq \langle \mu(t,x)\rangle = \int_{A_0} \langle m_0(\mathbf{a})\, \delta[t - \tau(x,\mathbf{a})]\rangle d\mathbf{a} = f(\tau,x) \tag{6}$$

where $f(\tau, x) = (1/U)\int V_x(\mathbf{a}) g[V_x(\mathbf{a}), \tau(x, \mathbf{a})] dV_x$ is the marginal pdf of traveltime at CP at x, whereas $g[V_x(\mathbf{a}), \tau(x, \mathbf{a})]$ is the bivariate pdf of velocity at the injection plane and the traveltime at the CP (for a detailed discussion in the frame of first-order analysis, see *Cvetkovic and Dagan* [1994]. In simple words (6) implies that the one realization mean solute flux over the CP is close to the ensemble pdf of one particle traveltime and the BTC is close to the cdf of τ, respectively. This equivalence is employed in P2 in order to compute various moments toward comparison with the numerical simulations. Under ergodic conditions we get for the different moments in (4): $T(x) \simeq \langle\tau(x)\rangle = \int \tau\, f(\tau, x) d\tau$, $\sigma_t^2(x) \simeq \sigma_\tau^2(x)$, $S_t(x) \simeq S_\tau(x)$. Whether μ and these moments display an ergodic behavior is one of the main issues investigated in the following and in P2.

[25] In a similar manner $m(t, x) \simeq \langle m(t, x)\rangle = f(x, t)$ in (5), where $f(X, t)$ is the marginal pdf of the longitudinal particle displacement X at time t. The various spatial moments of the plume were expressed mostly with the aid of the displacement moments in the past [e.g., *Dagan*, 1989]. For reasons of both numerical and analytical convenience, we rely here on the temporal representations.

2.2. Gaussianity and Equivalent Longitudinal Dispersivity

[26] If m (5) satisfies the ADE equation

$$\frac{\partial m}{\partial t} + U\frac{\partial m}{\partial x} = \alpha_L U \frac{\partial^2 m}{\partial x^2} \tag{7}$$

where the longitudinal dispersivity α_L is a function of the traveltime t, longitudinal transport is coined here as Gaussian. With the initial condition $m(0, x) = \delta(x)$, the well known solution for M (1) is

$$M(t,x) = \frac{1}{2}\mathrm{erfc}\left[\frac{x - Ut}{\left(4U\int_0^t \alpha_L(t')\,dt'\right)^{1/2}}\right] \tag{8}$$

[27] Previous studies have shown that after a sufficiently long time, denoted as "setting time" [*Fiori et al.*, 2003], m indeed tends to Gaussianity by virtue of the central limit theorem, while α_L tends to a constant value $\alpha_{L\infty}$. At this limit transport is coined as Fickian and then

$$\mu(t,x) = \frac{\partial M}{\partial t} = \frac{1}{2}\left(\frac{x}{t} + U\right) Z\left(\frac{x - Ut}{4\alpha_{L\infty}Ut}\right) \;;$$
$$Z\left(\frac{x - Ut}{4\alpha_{L\infty}Ut}\right) = \frac{1}{(4\pi\alpha_{L\infty}Ut)^{1/2}}\exp\left[-\frac{(x - Ut)^2}{4\alpha_{L\infty}Ut}\right] \tag{9}$$

[28] Furthermore, for $x \gg \alpha_{L\infty}$, we get from (9) for the temporal moments (4)

$$T = (x + \alpha_{L\infty})/U \simeq x/U;$$
$$\sigma_t^2 = \left(2\alpha_{L\infty}x + 5\alpha_{L\infty}^2\right)/U^2 \simeq (2\alpha_{L\infty}x)/U^2; \tag{10}$$

$$S_t = 4\alpha_{L\infty}^{1/2}\frac{3x + 11\alpha_{L\infty}}{(2x + 5\alpha_{L\infty})^{3/2}} \simeq [(18\alpha_{L\infty})/x]^{1/2} \tag{11}$$

[29] In a simple minded analysis of measured BTC in laboratory or in the field it is customary to identify an equivalent macrodispersivity with the aid of the temporal moments (11) even if transport is neither Gaussian nor Fickian, i.e.,

$$\alpha_{Leq} = \frac{\sigma_t^2 U^2}{2x} \tag{12}$$

and we shall adopt this measure as well in the analysis of numerical simulations.

2.3. Anomalous Behavior

[30] The subject of anomalous transport was investigated extensively in the physics literature [e.g., *Bouchaud and Georges*, 1990] and was considered also in the context of transport through heterogeneous porous formations. By Taylor theory [*Taylor*, 1921] and under ergodic conditions the macrodispersivity is proportional to the integral of the Lagrangian velocity covariance. If the latter has a finite integral scale, macrodispersivity tends to a constant value for sufficiently large traveltime and transport becomes Fickian. Similarly, by the central limit theorem, it tends to Gaussianity, though possibly at a slower rate. If the covariance is not integrable, the macrodispersivity grows indefinitely with time and transport is coined as anomalous. In the context of solute transport by groundwater, anomalous behavior has been attributed in the past mainly to the lack of a finite integral scale of the log conductivity covariance [e.g., *Dagan*, 1991; *Di Federico and Neuman*, 1998].

[31] In the case of the present structural model, in which Y has a finite integral scale, we know that under ergodic conditions and by the central limit theorem, transport has to become Fickian at large traveltime (which we coined as the "setting time"). However, for highly heterogeneous formations, this limit may be attained for large travel distances from the source, of order of hundreds of integral scales, and even more so, of thousands of integral scale for tendency to Gaussianity [*Fiori et al.*, 2003]. In hydrological applications this may be beyond the boundaries of the aquifer or the region in which it displays a stationary behavior. Therefore the issue of anomalous behavior for very large traveltime (or distance) from the source may become of a rather theoretical interest (this issue has been discussed recently for 2-D simulations by *Trefry et al.* [2003].

[32] In the present study, like in the case of ergodicity, we adopt a heuristic approach and regard transport as displaying anomalous behavior if the equivalent macrodispersivity (12) does not level off within the considered distance covered by the plume. Hence whether we regard transport as anomalous or not depends on the travel distance, on σ_Y^2, and on the size of the plume.

3. Numerical Simulations

[33] Three numerical simulations were carried out using 100,000 spherical inclusions placed in a flow domain shaped as an elongated prolate ellipsoid (Figure 1). The ellipsoid is $220I$ long (in x direction) and $110I$ wide (in y and z directions). The inclusions, placed on a face-centered cubic lattice at highest density, cover 70% of the ellipsoid volume ($n = 0.7$). Log conductivity of inclusions follows a normal distribution with variance values $\sigma_Y^2 = 2$, 4 and 8. The homogeneous background extends to infinity with conductivity that equals effective medium conductivity K_{ef}. The latter was found previously [*Janković et al.*, 2003a] to be equal to $1.291K_G$, $1.558K_G$ and $2.095K_G$ for $\sigma_Y^2 = 2$, $\sigma_Y^2 = 4$ and $\sigma_Y^2 = 8$, respectively. Comparison between the space averaged log conductivity autocorrelation ρ_Y and the theoretical one show close agreement (Figure 2) and consequently $R = (3/4)\,I$ [*Dagan*, 1989].

[34] The conglomerate of inclusions was subject to uniform flow from infinity of intensity U in x direction. The ellipsoidal geometry ensures uniform mean flow inside the flow domain. Since background conductivity was set to the effective conductivity, the uniform mean flow inside the domain has the same orientation and intensity as flow at infinity. This is revealed by the undisturbed planes of constant head outside the ellipsoid (Figure 1).

[35] The flow problem was solved using the analytic element method, by expanding the perturbation potential associated with each inclusion in series of spherical harmonics with unknown coefficients [*Janković and Barnes*, 1999]. The conservation of mass is obeyed exactly, whereas that of continuity of the head at the boundaries between inclusions and the matrix is satisfied with high accuracy, by solving with 289 degrees of freedom associated with each spherical inclusion. The formulation details are presented by *Janković et al.* [2003b]. The large number of degrees of freedom permits precise computation of disturbance potentials (associated with spherical inclusions) and corresponding velocities regardless of the medium heterogeneity and packing density. Simulations were carried out

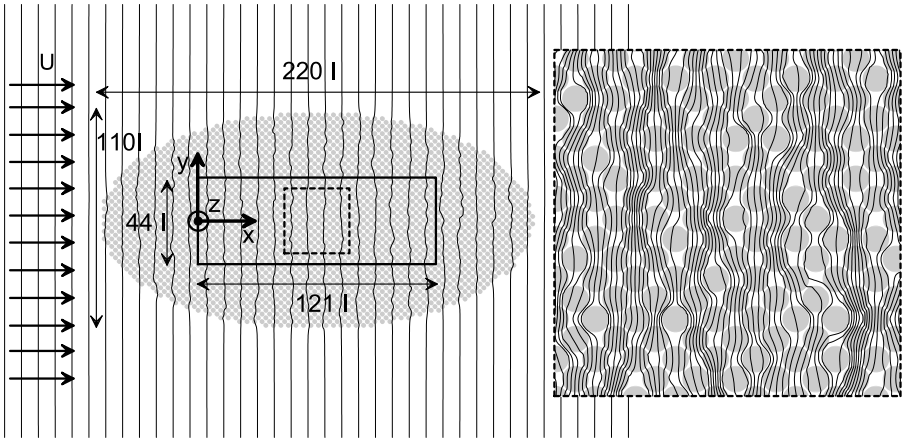

Figure 1. Schematic representation of the flow and transport domains. Lines normal to the mean flow direction are intersections of constant head surfaces and the plane $z = 0$.

on a massively parallel supercomputer cluster in the Center for Computational Research, University at Buffalo. Each simulation was run on 128 dual-processor Pentium 4 machines on cluster Joplin. The run times necessary to compute 2.89×10^7 coefficients depended on the σ_Y^2. For $\sigma_Y^2 = 8$, the single-processor equivalent run time was over 2,000 CPU days.

[36] Following the flow solution, the advective transport was simulated in a stationary core placed inside the flow domain (Figure 1). The core, shaped as a parallelepiped $121I$ long (in x direction) and $44I$ wide (in y and z directions), was smaller than the flow domain to eliminate nonstationary effects that are present in the zone near the flow domain boundary. Breakthrough curve for each control plane is computed by tracing 40,000 particles released at the upstream boundary ($x = 0$) of the stationary core with uniform spacing of $0.22I$ (in y and z directions). Details of the particle tracking algorithm are presented by *Janković et al.* [2003b].

4. Results of Numerical Simulations

[37] The numerical simulations permitted us to depict the relative mass flux μ (2) as function of t, for any fixed CP at x and for given log conductivity variance σ_Y^2. This is the most detailed type of information we are going to use in order to analyze data. To illustrate the results, we display in Figure 3 three such distributions for a distant CP (at $x/I = 116$) and for $\sigma_Y^2 = 2$ (Figure 3a), $\sigma_Y^2 = 4$ (Figure 3b) and $\sigma_Y^2 = 8$ (Figure 3c), respectively.

[38] It is seen that at the early arrival times, the mass flux displays the usual BTC behavior, similar to that pertaining to weak heterogeneity. The striking feature, that is related to high heterogeneity, is the presence of a very long tail for late times. This late arrivals of solute particles are caused by the long residence times in inclusions of low K (a detailed analysis is given in P2). The tail is amplified in the windows of Figure 3 and it is seen that for very low mass flux, less than say $0.01\mu_{max}$, the tail persists for traveltimes from the source of order of hundreds of I/U, depending on σ_Y^2. The oscillations in the tail are influenced by the size of the sampling intervals Δt and the corresponding numbers of particles that represent each interval. The selected interval size (that was in the range $0.7 \leq U\,\Delta t/I \leq 2.2$) only affects the graphical results presented in Figure 3. The main findings of this paper, contained in the Figures 4–7, are not affected by the selected interval size. Graphs depicting $\mu(t, x)$ for different x/I (not shown), display similar features.

[39] The tail encapsulates a minute portion of the total mass M_0 that is left behind the CP and it has little effect on the mean traveltime T (11). The latter was found to be close to the theoretical value x/U. In contrast, the tail has a large impact on the second and higher-order temporal moments. To illustrate this point we have computed the equivalent longitudinal macrodispersivity (12), based on the traveltime variance as derived from μ and its equivalence with the pdf of τ (6). Furthermore, the equivalent longitudinal macrodispersivity is determined as function of the time of integration t_I as follows

$$\alpha_{Leq}(t_I, x) = \frac{U^2}{2x} \int_0^{t_I} (t - T)^2 \mu(t, x)\, dt \quad ; \quad T = \frac{x}{U} \tag{13}$$

[40] From a theoretical standpoint the equivalent macrodispersivity at x is given by $\alpha_{Leq}(x) = \lim_{tI \to \infty} \alpha_{Leq}(t_I, x)$. The result is shown in Figure 4 for the numerically

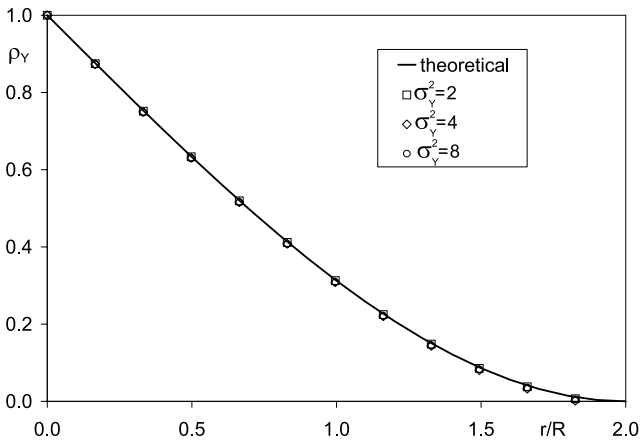

Figure 2. Theoretical log conductivity autocorrelation $\rho_Y = 1 - 3/(4R) + r^3/(8R^3)$ [*Dagan*, 1989] and the space-averaged values for the three realizations of the medium (r is the lag and R is the spheres radius).

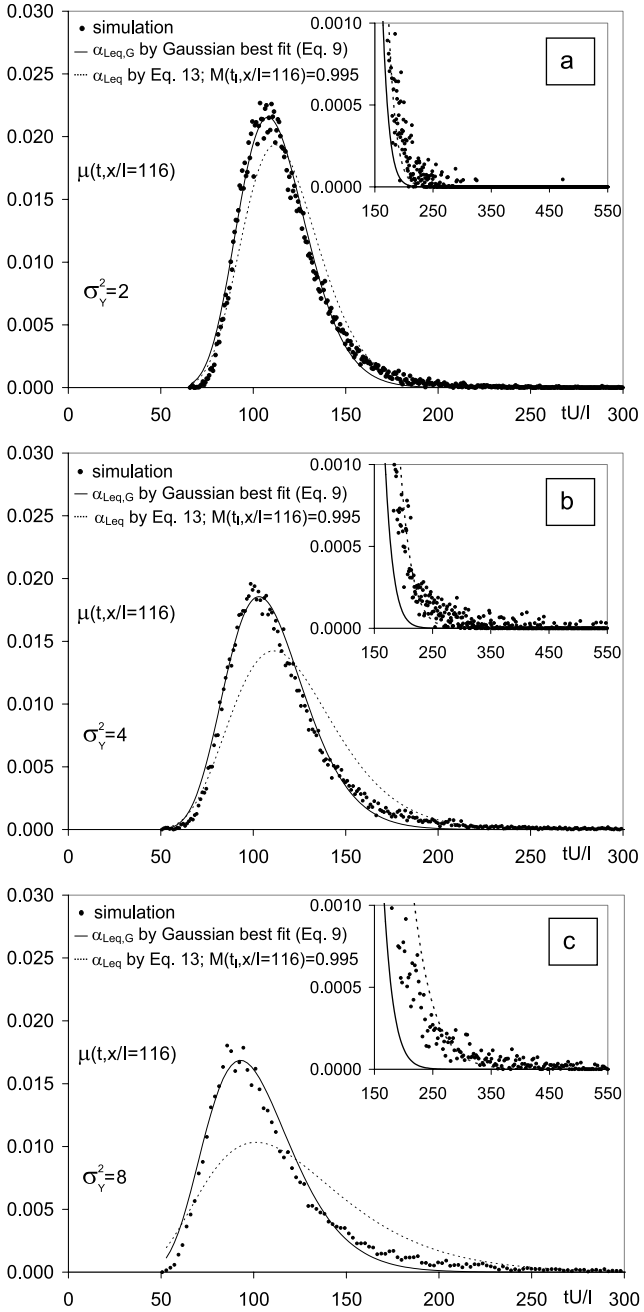

Figure 3. Numerically determined relative mass flux μ and the Gaussian distributions with equivalent macrodispersivity derived by best fit and by temporal moments of the simulated μ: (a) $\sigma_Y^2 = 2$, (b) $\sigma_Y^2 = 4$, and (c) $\sigma_Y^2 = 8$.

determined $\mu(t, x)$ of Figure 3c, i.e., for $x/I = 116$ and $\sigma_Y^2 = 8$. Macrodispersivity is made dimensionless with respect to the inclusions density $n = 0.7$, the variance σ_Y^2 and the integral scale I, in line with the first-order analysis that predicts $\alpha_{Leq}/(n\sigma_Y^2 I) \rightarrow 1$ for $x/I \gg 1$ [*Fiori et al.*, 2003]. The striking result is that indeed the tail influences $\alpha_{Leq}(t_I, x)$ for integration time in (13) as large as $1700I/U$. Furthermore, $\alpha_{Leq}(t_I, x)$ is fluctuating and the jumps apparent in Figure 4 are related to the passage of two or even one particle among the injected 40,000 ones. To further illustrate the effect of the tail we show in Figure 5 the effect of a cutoff by limiting

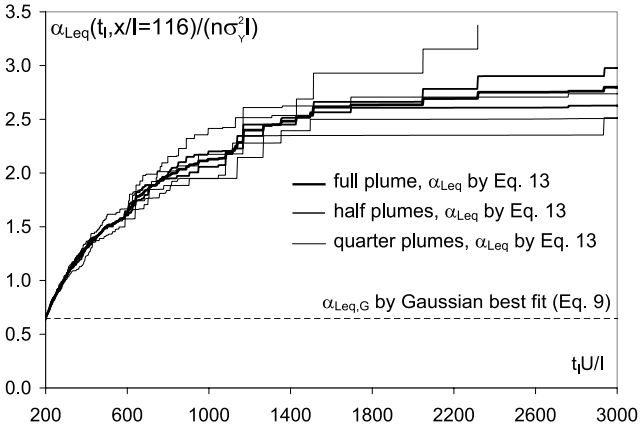

Figure 4. Numerically determined equivalent macrodispersivity α_{Leq} (13) based on the simulated mass flux μ, as function of the integration time t_I, for $x/I = 116$ and $\sigma_Y^2 = 8$. Results are shown for the full plume (injection area A_0), for half plumes ($A_0/2$), and quarter plumes ($A_0/4$).

t_I to the time of passage of 0.999 and 0.995 of the total mass, leading to $Ut_I/I \simeq 800$ and $Ut_I/I \simeq 400$, respectively. It is seen that the effect is to reduce the value of α_{Leq} to half or less (see P2).

[41] As we shall show in P2, the "latecomer" solute particles making up the tail are related to the long residence time in inclusions of very low K. The large spatial domain covered by the plume notwithstanding, the number of such inclusions may be quite small and dependent on the initial plume size, even though $A_0/I^2 = 2000$. To illustrate this point we further display in Figure 4 the same $\alpha_{Leq}(t_I, x)$ but this time for $\mu(t, x)$ based on two halves of the plume, i.e., $(1/2)A_0$ each, as well as for four quarters $(1/4)$ A_0. If transport were ergodic, the result for $\alpha_{Leq}(t_I, x)$ would have been weakly dependent on these relatively large sized subplumes and this indeed happens for say $t_I U/I < 300$ (see the low value of μ for this time in Figure 3c). However, for larger times the value of $\alpha_{Leq}(t_I, x)$ is dependent on the plume size.

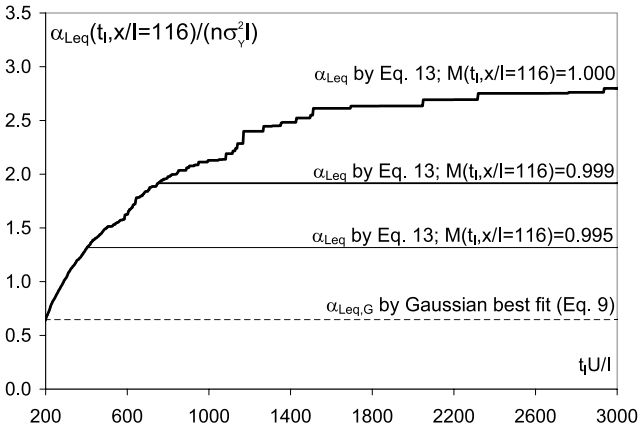

Figure 5. Numerically determined equivalent macrodispersivity α_{Leq} (13) based on the simulated mass flux μ for integration times t_I corresponding to the full mass recovery ($M = 1$), to partial ones ($M = 0.999$ and $M = 0.995$), and to Gaussian fits.

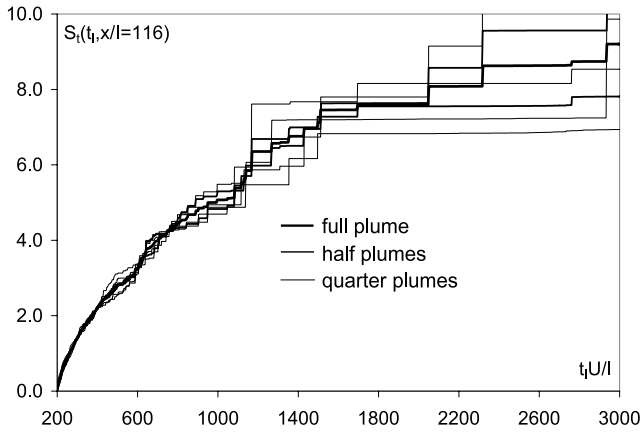

Figure 6. Numerically determined skewness (14) based on the simulated mass flux μ, as function of the integration time t_I, for $x/I = 116$ and $\sigma_Y^2 = 8$. Results are shown for the full plume (injection area A_0), for half plumes ($A_0/2$), and quarter plumes ($A_0/4$).

[42] The same effects are illustrated in Figure 6, which depict the skewness

$$S_t(t_I, x) = \frac{1}{\sigma_t^3}\int_0^{t_I} (t-T)^3 \mu(t,x)\, dt \quad ; \qquad T = \frac{x}{U} \quad ; \quad \sigma_t^2 = \int_0^{t_I} (t-T)^2 \mu(t,x)\, dt \tag{14}$$

as function of t_I and the plume size. As expected, skewness is influenced even in a more dramatic way by the tail persistence.

[43] Summarizing the findings at this point, we conclude that for highly heterogeneous formations: (1) the mass flux distribution is highly skewed due the presence of a "thin" but persistent tail, (2) the traveltime variance and the corresponding equivalent longitudinal macrodispersivity, as well as the skewness, depend significantly on the cutoff of the tail, even at very large times, after the arrival of most of the mass and (3) in spite of the ergodic behavior that was expected for the selected large injection area, the second and higher temporal moments display a nonergodic behavior. Hence ergodic behavior is dependent not only on the plume transverse size and on σ_Y^2, but also on the observation time t_I. This is a subtle effect, that to the best of our knowledge was not detected in previous numerical simulations. Needless to say that additional factors not considered here, e.g., molecular diffusion, poor characterization of the log conductivity pdf at extreme values, possible measurement errors etc, are further increasing the uncertainty of the tail behavior.

[44] In many conceivable applications the main interest resides in the large concentrations pertinent to most of the mass flux function μ, and much less in the behavior of the tail. As we have seen the mass arrival displays an ergodic behavior and a reduction of the skewness if a cutoff t_I is applied. We adopt such a cutoff in an indirect manner by approximating the numerically determined μ (Figure 3) by the Gaussian expression (9) in which U is replaced by $U_{eq,G}$ and $\alpha_{L\infty}$ is by $\alpha_{Leq,G}$. This is the procedure that would be applied by an experimentalist that measures the BTC: approximating it by the solution of the ADE with constant coefficients (7) and deriving the equivalent velocity and macrodispersivity by a best fit.

[45] We have applied this procedure to the entire mass flux functions $\mu(t, x)$ determined from the numerical simulations and by a least squares fit. The problematic tail has a minimal impact upon the fitted $\alpha_{Leq,G}$ and as a matter of fact the simulated curve is modeled quite accurately by (9), as shown in Figure 3. The values of $\alpha_{Leq,G}$ thus obtained are displayed in Figures 4 and 5 and they are much lower than the ones based on (12) for $M = 1$, $M = 0.999$ and $M = 0.995$, respectively. This is also demonstrated by using the theoretical value $\alpha_{Leq} = \sigma_t^2 U^2/2x$ (12) for $M = 0.995$ in the Gaussian expression (9), leading to a poor fit with the mass flux distribution (Figure 3). As expected, the discrepancy between μ in the numerical simulations and the two Gaussian fits increases with the heterogeneity degree. The fact that approximating the mean longitudinal mass distribution of the plume and the corresponding BTC by a Gaussian one may reproduce quite accurately most of the distribution, except of course the persistent tail, is an encouraging finding as far as applications are concerned. The relationship between the fitted $U_{eq,G}$ and $\alpha_{Leq,G}$ and the structural parameters is discussed in P2.

[46] Finally, we represent the dependence of the equivalent macrodispersivity upon the distance x from the source in the summarizing graphs of Figure 7. In view of the above discussion, the values (13) based on the numerically determined μ depend on the cutoff of arrived mass and there is no unique equivalent macrodispersivity for a given x. Consequently, we display the result for almost full recovery of mass $M = 0.999$, for $M = 0.995$, as well as for the Gaussian fit (9). It is seen that the reduction effect of the cutoff manifests over the entire domain. Furthermore, equivalent macrodispersivity does not seem to level off in the considered interval for the highest $\sigma_Y^2 = 8$ and it may be perceived as anomalous. There is an apparent tendency to Fickianity of equivalent macrodispersivity for lower σ_Y^2, but after travel distances of tens of integral scales.

5. Summary and Discussion

[47] Flow and transport in three-dimensional highly heterogeneous formations are solved numerically. The medium

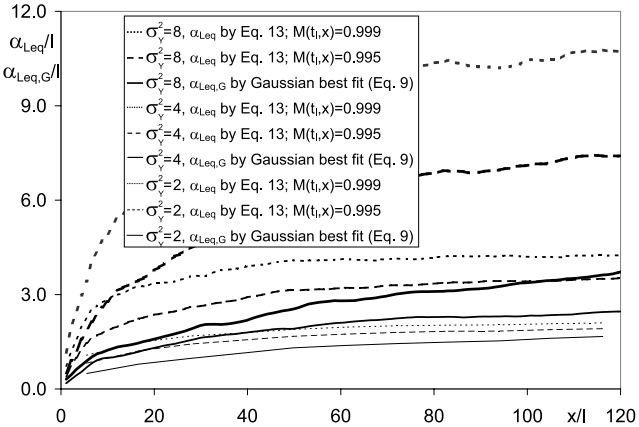

Figure 7. Dependence of the equivalent macrodispersivity on the distance from the injection plane.

is modeled as a collection of spherical blocks of uniform radius R that are packed at maximum density $n = 0.7$ and are submerged in a matrix of conductivity equal to K_{ef}. The inclusions' conductivities are random and independent, of a lognormal distribution. The isotropic medium is completely characterized by the conductivity geometric mean K_G, the log conductivity variance σ_Y^2 and the integral scale $I = (3/4)R$. Three realizations with $\sigma_Y^2 = 2, 4, 8$, respectively, are computer simulated and flow is solved with high accuracy by the analytic element method. A thin plume is injected instantaneously in the plane $x = 0$, normal to the mean uniform flow of velocity U. The initial area $A_0 \simeq 2000I^2$ is very large in comparison to the values adopted in previous works. The injection mode is flux proportional and the solute particles are advected (diffusion and pore-scale dispersion are neglected) by the fluid. Longitudinal transport is analyzed with the aid of the relative solute mass flux $\mu(t, x)$ at control planes at fixed x ($x_{\max} \simeq 121I$). Under ergodic conditions (that were expected for the given large transverse size of the plume) μ is equal to the pdf of traveltime $f(\tau, x)$ of a solute particle moving from $x = 0$ to x.

[48] The main finding about transport in highly heterogeneous formations, in contrast with the weakly heterogeneous ones, is that μ displays a thin, but persistent, tail which is caused by solute particles that move very slowly from the injection to the control plane. In contrast, the arrival of the faster moving solute, making up the bulk of the plume, displays a Gaussian-like shape. The tail comprises a small part of the total mass and it does not affect the mean traveltime $T = x/U$. It has however a large impact on the second and on higher temporal moments. The latter are sensitive to a cutoff of μ, even for times for which 0.995 of the mass has moved past the control plane. Thus an equivalent macrodispersivity based on the second temporal moment may change by a factor of 2, depending on the cutoff and even more so for the skewness.

[49] In spite of the large transverse size of the simulated initial plume, the tail of μ is not ergodic: it fluctuates at large traveltime and it is dependent on the size of A_0. This subtle effect, that was not revealed previously, is related to the presence of blocks of low permeability (see P2). In view of this nonergodic behavior, of the imprecise characterization of the log conductivity pdf in hydrological applications, of measurement errors and of the neglect of molecular diffusion, it seems to us that modeling and prediction of the tail of μ, though of theoretical interest, may be of little use in practice. Hence risk assessment relying on such predictions are highly imprecise and the use of a macrodispersion coefficient based on the second moment is questionable.

[50] The positive finding is that the mass arrival of the bulk of the plume, say above 95% of the total, can be described by a Gaussian model, with equivalent mean velocity $U_{eq,G}$ and longitudinal dispersivity $\alpha_{Leq,G}$, which were determined by a least squares fit of the Gaussian distribution and the simulated μ. The latter is captured quite accurately by the Gaussian model, except of course for the tail. For weak heterogeneity, say $\sigma_Y^2 < 1$, the entire plume is close to Gaussian, and $U_{eq,G} \simeq U$ while $\alpha_{Leq,G} \simeq \alpha_L$ can be determined by theoretical models, e.g., by a first-order approximation in σ_Y^2. The derivation of equivalent macrodispersivity with the aid of simple models for highly heterogeneous formations is a challenging task (see P2). It is emphasized that both $U_{eq,G}$ (see Figure 7a of P2) and $\alpha_{Leq,G}$ (Figure 5) are nonlocal as they depend on the traveltime from the source, for a large period depending on σ_Y^2.

[51] Finally, it seems that for the largest $\sigma_Y^2 = 8$, the equivalent macrodispersivity, determined either from the second temporal moments based on μ with a cutoff or from the Gaussian fit, does not level off with x within the considered domain ($x \leq 121I$). Hence the transport appears as anomalous, though on theoretical grounds it should become Fickian after a sufficiently long travel distance. This finding (which was set forth in our previous work [*Janković et al.*, 2003a, 2003b] and for 2-D flow by *Trefry et al.* [2003], although for smaller x) suggests that anomalous behavior is not intrinsic and dependent only on the structure, but also on the modeled interval. Hence the question on whether transport is Fickian or not asymptotically may be of theoretical interest, but again of limited practical relevance for such large σ_Y^2, since it applies to extremely large travel distances, possibly beyond the formation boundary or the domain of stationarity of the conductivity. Transport is closer to Fickianity for the smaller σ_Y^2 as far as equivalent macrodispersivity is concerned, but skewness is still large for the entire μ distribution.

[52] These findings, as well as the difficulty of characterizing the spatial distribution of permeability in the field, pose challenging problems to modeling contaminant transport in highly heterogeneous formations of a three-dimensional structure.

[53] **Acknowledgments.** This paper is based upon work partially supported by the National Science Foundation under grant EAR-0218914. The authors also wish to thank the Center for Computational Research, University at Buffalo, for resources and assistance in running numerical simulations.

References

Bellin, A., P. Salandin, and A. Rinaldo (1992), Simulation of dispersion in heterogeneous porous formations: Statistics, first-order theories, convergence of computations, *Water Resour. Res.*, *28*, 2211–2228.

Bouchaud, J. P., and A. Georges (1990), Anomalous diffusion in disordered media: Statistical mechanisms, models and physical applications, *Phys. Rep.*, *195*, 127–229.

Chin, D. A. (1997), An assessment of first-order stochastic dispersion theories in porous media, *J. Hydrol.*, *199*, 53–73.

Cvetkovic, V., and G. Dagan (1994), Transport of kinetically sorbing solute by steady random velocity in heterogeneous porous formations, *J. Fluid Mech.*, *265*, 189–215.

Cvetkovic, V., and G. Dagan (1996), Reactive transport and immiscible flow in geological media. II. Applications, *Proc. R. Soc. London, Ser. A.*, *452*, 303–328.

Cvetkovic, V. D., and A. M. Shapiro (1990), Mass arrival of sorptive solute in heterogenous porous media, *Water Resour. Res.*, *26*, 2057–2067.

Dagan, G. (1989), *Flow and Transport in Porous Formations*, Springer, New York.

Dagan, G. (1991), Dispersion of a passive solute in non-ergodic transport by steady velocity fields in heterogeneous formations, *J. Fluid. Mech.*, *233*, 197–210.

Dagan, G., A. Fiori, and I. Janković (2003), Flow and transport in highly heterogeneous formations: 1. Conceptual framework and validity of first-order approximations, *Water Resour. Res.*, *39*(9), 1268, doi:10.1029/2002WR001717.

Demmy, G., S. Berglund, and W. Graham (1999), Injection mode implications for solute transport in porous media: Analysis in a stochastic Lagrangian framework, *Water Resour. Res.*, *35*, 1965–1973.

Di Federico, V., and S. P. Neuman (1998), Transport in multiscale log conductivity fields with truncated power variograms, *Water Resour. Res.*, *34*, 963–973.

Fiori, A., I. Janković, and G. Dagan (2003), Flow and transport in highly heterogeneous formations: 2. Semianalytical results for isotropic media, *Water Resour. Res.*, *39*(9), 1269, doi:10.1029/2002WR001719.

Fiori, A., I. Janković, and G. Dagan (2006), Modeling flow and transport in highly heterogeneous three-dimensional aquifers: Ergodicity, Gaussianity, and anomalous behavior—2. Approximate semianalytical solution, *Water Resour. Res.*, *42*, W06D13, doi:10.1029/2005WR004752.

Gelhar, L. W. (1994), *Stochastic Subsurface Hydrology*, 390 pp., Prentice-Hall, Upper Saddle River, N. Y.

Janković, I., and R. Barnes (1999), Three-dimensional flow through large numbers of spherical inhomogeneities, *J. Hydrol.*, *226*, 224–233.

Janković, I., A. Fiori, and G. Dagan (2003a), Effective conductivity of an isotropic heterogeneous medium of lognormal conductivity distribution, *SIAM J. Multiscale Model. Simul.*, *1*(1), 40–56.

Janković, I., A. Fiori, and G. Dagan (2003b), Flow and transport in highly heterogeneous formations: 3. Numerical simulations and comparison with theoretical results, *Water Resour. Res.*, *39*(9), 1270, doi:10.1029/2002WR001721.

Rinaldo, A., A. Marani, and A. Bellin (1989), On mass response functions, *Water Resour. Res.*, *25*, 1603–1617.

Rubin, Y. (2003), *Applied Stochastic Hydrology*, 391 pp., Oxford Univ. Press, New York.

Salandin, P., and V. Fiorotto (1998), Solute transport in highly heterogeneous aquifers, *Water Resour. Res.*, *33*, 949–961.

Strack, O. D. L. (1989), *Groundwater Mechanics*, Prentice-Hall, Upper Saddle River, N. J.

Taylor, G. I. (1921), Diffusion by continuous movements, *Proc. London Math. Soc., Ser. A*, *20*, 196–211.

Tompson, A. F. B., and L. W. Gelhar (1990), Numerical simulation of solute transport in three-dimensional, randomly heterogeneous media, *Water. Resour. Res.*, *26*, 2541–2562.

Trefry, M. G., F. P. Ruan, and D. McLaughlin (2003), Numerical simulations of preasymptotic transport in heterogeneous porous media: Departures from the Gaussian limit, *Water Resour. Res.*, *39*(3), 1063, doi:10.1029/2001WR001101.

Wen, X. H., and J. J. Gomez-Hernandez (1998), Numerical modeling of macrodispersion in heterogeneous media: A comparison of multi-Gaussian and non-multi-Gaussian models, *J. Contam. Hydrol.*, *30*, 129–156.

Zinn, B., and C. F. Harvey (2003), When good statistical models of aquifer heterogeneity go bad: A comparison of flow, dispersion, and mass transfer in connected and multivariate Gaussian hydraulic conductivity fields, *Water Resour. Res.*, *39*(3), 1051, doi:10.1029/2001WR001146.

G. Dagan, Faculty of Engineering, Tel Aviv University, Ramat Aviv, 69978 Tel Aviv, Israel. (dagan@eng.tau.ac.il)

A. Fiori, Dipartimento di Scienza dell'Ingegneria Civile, Universita' di Roma Tre, Via Volterra 62, I-00146 Rome, Italy. (aldo@uniroma3.it)

I. Janković, Department of Civil, Structural and Environmental Engineering, State University of New York at Buffalo, Buffalo, NY 14260-4400, USA. (ijankovi@eng.buffalo.edu)